Increasing and enhancing the performance and antifouling characteristics of PES membranes using acrylic acid and microwave-modified chitosan

Yaghoub Mansourpanah[*,**,†], **Ali Kakanejadifard**[*], **Fatemeh Goudarzi Dehrizi**[*],
Meisam Tabatabaei[**], **and Hamid Soltani Afarani**[*]

*Membrane Research Laboratory, Lorestan University, Khorramabad, Iran
**Membrane Separation Technology (MST) Group, Biofuel Research Team (BRTeam),
Agricultural Biotechnology Research Institute of Iran, Karaj, Iran

Abstract−The aim of this study was to coat and change the surface properties of the PES membranes to increase the membrane performance. Accordingly, we coated a layer of chitosan on a PES membrane and then modified the created layer by acrylic acid and microwave irradiation for the first time. The fabricated layer was modified by acrylic acid (AA) as a grafting agent using a household microwave apparatus without any initiator. Different concentrations of AA and irradiation power as well as irradiation times were studied for the purpose. The obtained membranes were characterized using SEM, AFM, ATR-FTIR, contact angle, cross flow filtration, and anti-fouling property measurements. SEM images showed both the formation of a chitosan-coated PES membrane under the procedure and the resultant alterations in the surface structure. Based on the results, a moderate concentration of AA could enhance the coated layer properties and the rejection capability as well as the antifouling properties of the obtained membranes. AFM images represented the changes in the nanostructure of the coated layers as well as the surface characteristics. Accordingly, the mean surface pore sizes of the obtained membranes were reduced down to 35 nm after modification calculated by SPM-DME software. The antifouling properties of the modified membranes using bovine serum albumin (BSA) as a protein pattern showed that the flux recovery ratio (FRR) of some membranes increased by three times more than that of the unmodified membrane.

Keywords: PES Modification, Coating, Chitosan, Fouling

INTRODUCTION

The membrane separation process has been used in many applications, such as pharmaceutical, chemical, paper, textile, industrial water production, wastewater treatment, water softening, and separation of compounds having different molecular weights. Many membranes developed to date have a thin film composite (TFC) structure because of some key advantages relative to asymmetric membranes. A composite membrane is obtained by forming an ultra-thin dense layer on a porous support layer [1,2]. In a TFC membrane, each layer can be optimized for its particular function. The thin active layer can be optimized for a desired combination of permeate flux and solute rejection, while the support layer can be optimized for desired mechanical strength with low resistance to permeate flow. Based on the literature, several processes like interfacial polymerization, coating, layer-by-layer assembly, and spray processing have been reported for preparing of TFC membranes [3,4].

Chitosan, a natural, biodegradable, biocompatible, bioadhesive polymer, is gaining attention for a wide range of polymer applications in different fields [5,6]. Chitosan is a copolymer of glucosamine and N-acetyl glucosamine linked by β 1-4 glucosidic bonds obtained by N-deacetylation of chitin. The molecular weight and

degree of deacetylation can be modified during its preparation to obtain tailor-made properties. Also, chitosan has free amine as well as hydroxyl groups, which can be modified to obtain different chitosan derivatives [7-10]. On the other hand, chitosan shows a few drawbacks, such as acidic solubility as well as low thermal and mechanical stability. Nevertheless, the presence of hydroxyl and amino groups in the chitosan matrix provides some appropriate sites for reaction with desirable chemical materials such as vinyl monomers [11-14]. Therefore, chitosan modification could offer a new range of properties and applications.

One powerful physical technique for organic synthesis is microwave application as it enhances the rates of some reactions over the rates obtained using conventional reactions [15,16]. Microwave has been industrially applied for some processes such as polymerization [17]. Microwave energy can be directly and uniformly absorbed throughout the entire volume of an object, causing it to heat evenly and rapidly [18]. It has been also used in the synthesis of chitosan-graft-poly (acrylonitrile) without any radical initiator to prepare a modified PES membrane [19-21]. In our previous work, we changed and modified a chitosan layer by acrylamide as a crosslinker reagent. Accordingly, a modified PES membrane was obtained by showing the remarkable changes in the properties while the rejection capability was low, yet [22].

Surface coating is a versatile way to prepare and modify the nanoporous membranes. In this study acrylic acid, containing a -COOH group in the structure and due to its different properties, was uti-

lized to investigate and follow the changes in the surface characteristics of the chitosan-modified PES membranes using microwave irradiation. Comprehensive literature review showed that no outstanding researches have been done to use AA to modify the chitosan layer coated on the PES membranes. Using this procedure, changes in the surface properties and performance of the obtained membranes due to the existence of different cross-linkers were anticipated. The performance and structure of a coating chitosan thin layer might be changed by modification procedure in the presence of acrylic acid as a modifier and microwave as an energy initiator. Characterization methods were utilized to illustrate the changes in morphology, structure and performance of the modified thin layers. Antifouling properties of the resulting thin layers were investigated to reveal whether the proposed modification procedure was successful.

EXPERIMENTAL

1. Materials and Apparatus

Polyethersulfone (PES Ultrason E6020P with MW=58,000 g/mol) was supplied by BASF Company (Germany). Polyvinylpyrrolidone (25,000 g/mol), dimethylformamide, polyethylene glycol 600, acrylic acid (AA), acetic acid and NaCl salt were purchased from Merck (Germany). NaCl was chosen to investigate the rejection capability of the membranes. Bovine serum albumin (BSA) powder (assay>96%, mol wt.; 66 kDa, pH≈7, solubility>40 mg/mL in H_2O), was obtained from Sigma. Chitosan (CS) was purchased from Fluka. Distilled water was used throughout the study.

2. Fabrication of PES Support

The PES support was prepared by dissolving 18 wt% of PES in dimethylformamide with 10 wt.% of Polyvinylpyrrolidone, 3 wt% of acrylic acid and 5 wt% of polyethylene glycol 600 as additives by stirring for 4 h at 50 °C. The stirring was carried out at 300 rpm. After formation of a homogeneous solution, the doped solution was held at the ambient temperature for around 4 h to remove the air bubbles. Afterwards, the doped solution was cast on non-woven polyester (with 150 μm thickness) at 150 μm height using a film applicator at room temperature and in 30% humidity without evaporation. After coating, the membrane was immersed into a distilled water bath for at least 24 h to guarantee complete phase separation.

3. Chitosan Thin Film Preparation

The PES support membrane was clamped between two Teflon frames (height: 0.7 cm high and, inner cavity: 7.5×20 cm²). The chitosan-modified PES membranes were prepared as follows.

Three grams of chitosan was dispersed in 1,000 g of 3% acetic acid solution at room temperature. The temperature was then raised to 60 °C to complete chitosan dissolution. The obtained solution was poured on top of the PES support membrane and was allowed to get wet for 60 min at ambient temperature. The surface was rolled by a soft roller to eliminate any little bubbles during the wetting procedure. After draining excess solution, the second solution (aqueous phase) of AA at different concentrations (1.8, 3, and 4.2 wt%) was poured into the holders. The membranes were immediately exposed to different irradiation powers (180, 360 and 540 W), for different times (10, 30 and 60 s). After 60 min, the excess solution was poured off and the membrane was exposed to hot air for 5 min

Table 1. The proposed levels for all variants

Variants	Levels		
Acrylic acid (%w/v)	1.8	3	4.2
Microwave irradiation power (W)	180	360	540
Radiation time (s)	10	30	60

Table 2. Composition of the obtained membranes

Name	Concentration of CS (wt%)	Irradiation power (W)	Concentration of AA (wt%)	Irradiation time (s)
F_0	0.3	0	0	0
F_1	0.3	180	1.8	10
F_2	0.3	180	3.0	30
F_3	0.3	180	4.2	60
F_4	0.3	360	3.0	10
F_5	0.3	360	4.2	30
F_6	0.3	360	1.8	60
F_7	0.3	540	4.2	10
F_8	0.3	540	1.8	30
F_9	0.3	540	3.0	60

at 70 °C. In this study, Taguchi design (orthogonal arrays) was used, which allowed analyzing many factors with fewer runs. Tables 1 and 2 show the proposed levels for all variants and the composition of the obtained membranes, respectively.

4. Characterization Methods

Chemical alteration of the membranes was investigated using an Equniox 55 Bruker FT-IR spectrometer (Germany), with an attenuated total reflection (ATR) attachment. The surface and cross-section of the membranes was examined by using a Philips scanning electron microscope (SEM). The atomic force microscopy (AFM, non contact mode) was used to analyze the surface morphology and roughness of the membranes. The AFM apparatus was a DualScope™ scanning probe-optical microscope (DME model C-21, Denmark). The static contact angles were measured using a contact angle measuring instrument (G10, KRUSS, Germany). Deionizer water was used as the probe liquid in all measurements and the contact angles between water and the membrane surface were measured for evaluation of the membrane hydrophilicity. To minimize the experimental error, the contact angle was measured at five random locations for each sample. The ion rejections were investigated by measuring the permeate conductivity using a conductivity meter (Hanna 8733 Model, Italy).

A batch cross flow system was used to investigate the performance of the prepared membranes (Fig. 1). The membrane surface area in the filtration cell was 22 cm². The flux of each membrane was determined at 10 min intervals under 0.8 MPa. The experiments were carried out at 25 °C. The cross flow velocity was approximately 0.6 m/s for all tests. The permeation rate and salt rejection were determined for all membranes using NaCl solution of 1,000 ppm concentration. The rejection was calculated by using Eq. (1):

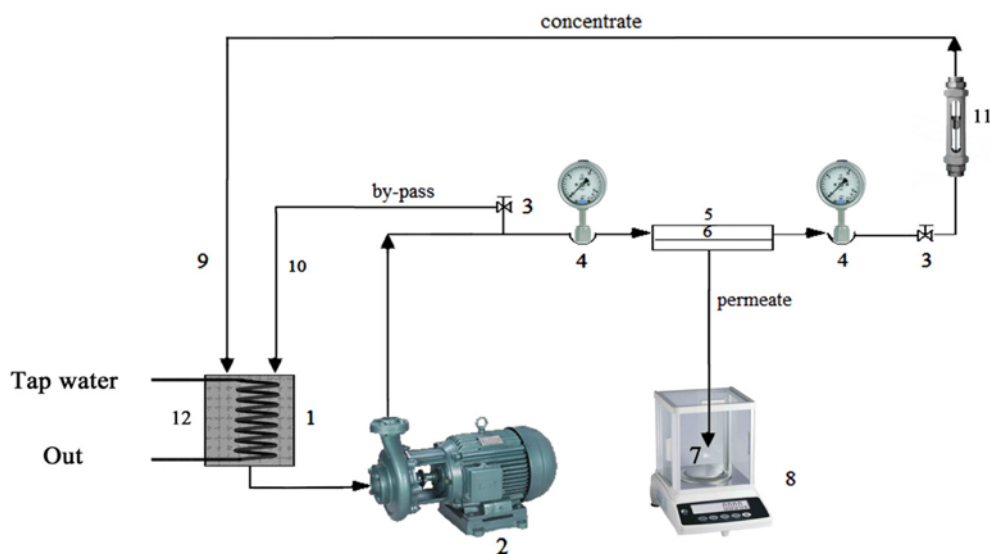$$R\% = \left[1 - \frac{\lambda_p}{\lambda_f} \right] \times 100 \tag{1}$$

Fig. 1. Cross-flow filtration set-up used to determine water permeation and salt rejection.

| 1. Feed tank | 3. Valve | 5. Cross flow cell | 7. Permeate | 9. Concentrate | 11. Flowmeter |
| 2. Pump | 4. Pressure guage | 6. Membrane | 8. Balance | 10. By-pass | 12. Cooling system |

where λ_p and λ_f are the ion conductivity in the permeate and feed, respectively [22].

Fouling can be quantified by taking into account the resistance appearing during the filtration, and cleaning can be specified by the removal of this resistance. The resistance is due to the formation of a cake or gel layer on the membrane surface. The flux (J) through the cake and the membrane may be described by Eq. (2):

$$J = \frac{m}{A \Delta t} \tag{2}$$

where m is the mass of the permeated water, A the membrane area, and Δt the permeation time [22].

After water flux measurement (J_{wi}), the solution reservoir was refilled with a 0.1 g/L BSA solution and the flux was obtained (J_p). After 2 h of filtration, the membrane was washed with deionized water for 10 min and the water flux of the cleaned membranes was measured (J_{wc}). To evaluate the fouling-resistance capability of the membrane, the flux recovery ratio (FRR) was calculated using Eq. (3):

$$FRR = \left(\frac{J_{wc}}{J_{wi}}\right) \times 100 \tag{3}$$

R_r and R_{ir}, described by Eqs. (4) and (5) show reversible deposition and irreversible fouling [23]:

$$R_r(\%) = \left(\frac{J_{wc} - J_p}{J_{wi}}\right) \times 100 \tag{4}$$

$$R_{ir}(\%) = \left(\frac{J_{wi} - J_{wc}}{J_{wi}}\right) \times 100 \tag{5}$$

RESULTS AND DISCUSSION

1. ATR-IR Analysis

CS is a large molecule composed of many hydroxide (-OH) and amino (-NH$_2$) groups. These groups attached to the large CS molecule may behave as if they were anchored to an immobile raft and its localized rotations [24]. Therefore, the microwave irradiation and resulting dielectric heating effect on the CS molecule could lead to an enhancement of reaction rates specifically at these groups. The dielectric heating will involve rapid energy transfer from these groups to existing molecules and water, since it is not possible to store the energy in a specific part of the molecule. Moreover, the dielectric heating results in breaking bonds creating radical sites at
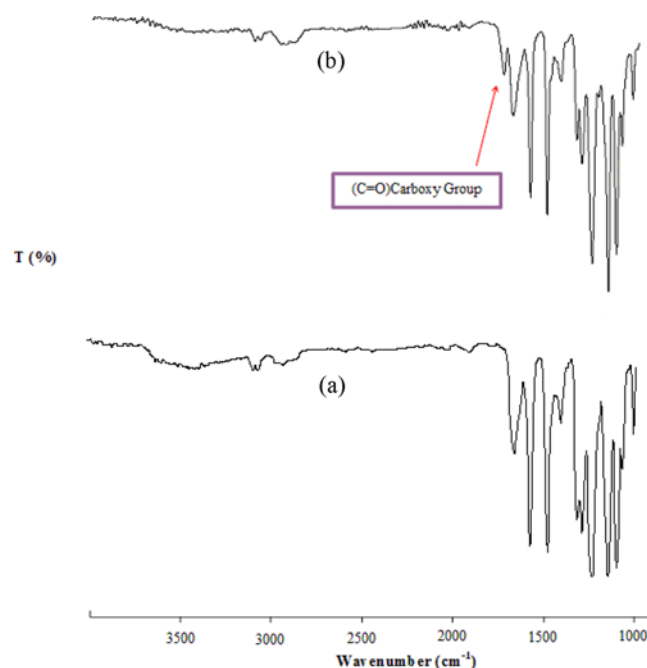

Fig. 2. ATR-IR spectrum of (a) the PES membrane and (b) the modified chitosan thin layer.

oxygen and nitrogen atoms. However, there will be a greater possibility for the formation of free radicals at nitrogen site as the bond energy of N-H bond is reported to be lower than that of the O-H bond. Furthermore, microwave radiation has also been reported to have a special effect on lowering Gibbs energy of activation, and in view of the two above effects, a plausible free radical mechanism for grafting under microwave irradiation has been proposed. More specifically, N-H bonds at CS absorb microwave energy and will cleave, generating monomer free radical and macro radical [25,26].

Fig. 2 presents the chemical structure of the PES membrane and chitosan-coated PES membrane. The ATR-IR spectrum indicates that the chitosan thin film was formed since a strong band at 1,722 cm^{-1} appeared. This is the characteristic of C=O band in the chitosan structure due to the grafting of AA. The peak at 1,293 cm^{-1} is assigned to C-N stretching. In addition, the observed peaks at 2,950 and 1,103 cm^{-1} assigned to C-H and C-O stretching bindings, respectively. However, due to the small amounts of reagents on the surface as modifiers and formation a very thin layer on the PES suppor, the peak intesity of the involved functions is weak.

2. Microscopy Characterization

To see the preparation of chitosan layer on the PES membranes, the membrane morphology including the surface and cross-section structures was visualized using SEM. As shown in Fig. 3(a), the PES membrane illustrated a quite smooth, flat and even surface structure which shows a bright surface. After coating the PES surface by chitosan, according to the procedure mentioned above, an uneven and a little bit dark more layer was formed over the PES membranes (Fig. 3(b)). Formation a chitosan layer over the PES membrane was clearly observed by cross-section images. These images clearly prove the creation a chitosan layer above the PES surface and are in agreement with the ATR-IR spectrum. Therefore, according to the SEM images, the process was successful to create a layer of chitosan over the PES membrane for changing the surface properties of the obtained membranes and improving their performance.

On the other hand, AFM images were used to better investigate and describe the effects of preparation conditions on the morphology of the obtained layers. There are many studies which gained AFM images to investigate the morphology and nano-scale changes of the membrane surfaces [27-30]. For this purpose, two membranes (F_1 and F_7) were chosen. These membranes were exposed to the same time of irradiation while its power and AA concentration were different: (180 W for F_1 and 540 W for F_7) and (1.8 w/v% for F_1 and 4.2 w/v% for F_7), respectively. Fig. 4 shows the AFM images of the chitosan layers by two- and three-dimensional surface images along with the image profile. The surface roughness parameters of the membranes, which are explained in terms of the mean roughness (S_a), the root mean square of the Z data (S_q) and the mean difference between the highest peaks and lowest valleys (S_z) as well as surface pore sizes, were calculated by SPM DME software and presented in Table 3. According to the data in Table 3
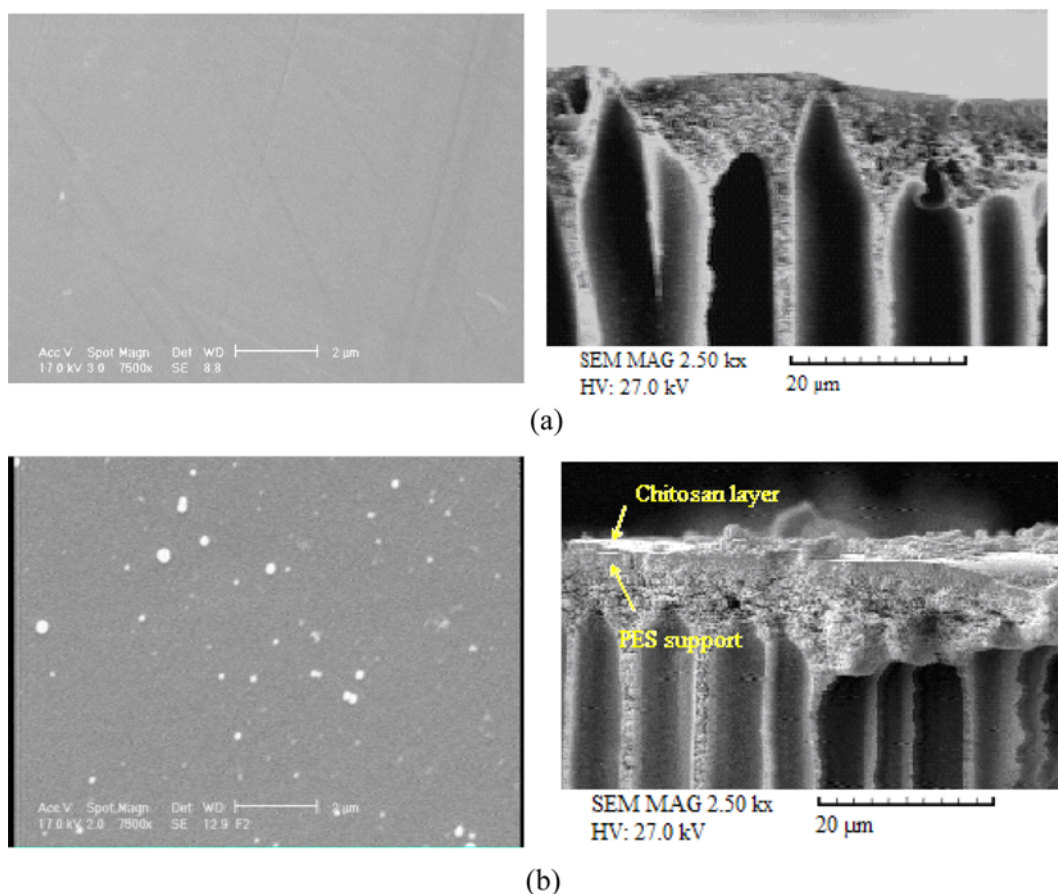

Fig. 3. SEM surface and cross-section images of (a) the PES membrane (b) the modified PES with chitosan.
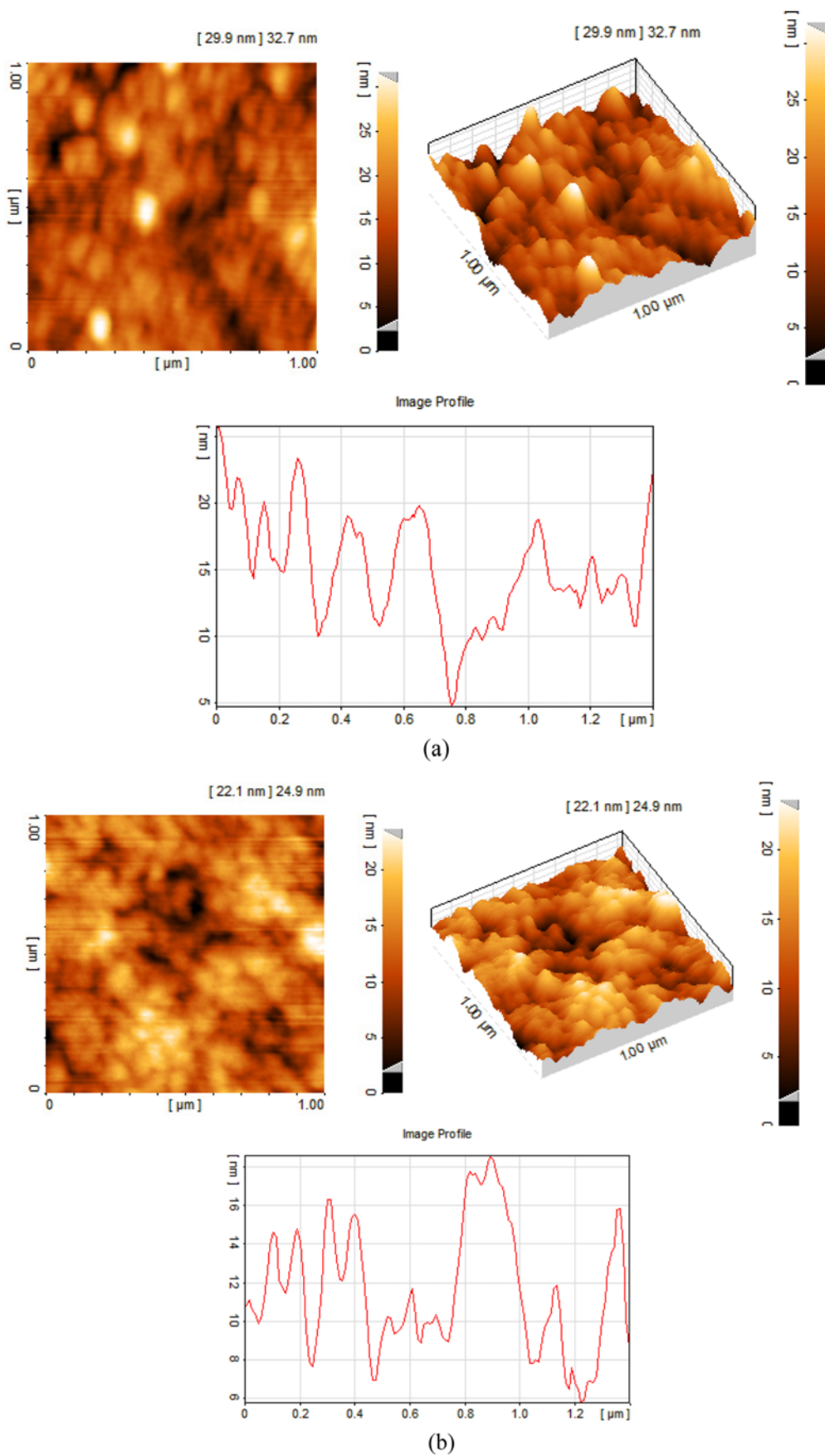
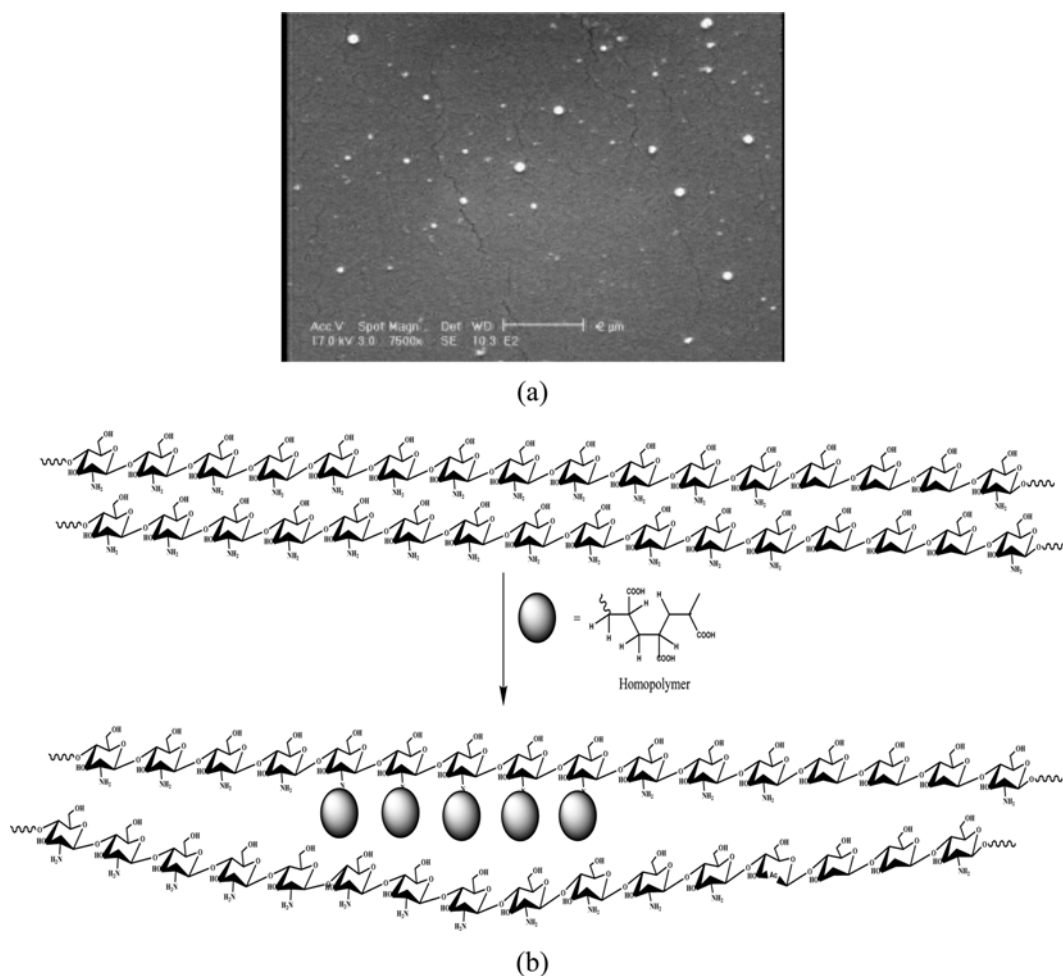Fig. 4. AFM surface images of the prepared membranes (a) F_1 and (b) F_7.

Table 3. The surface pore size and surface roughnesses parameters calculated using SPM software

Membrane	Mean surface pore size (nm)	Roughness parameters (nm)		
		S_a	S_q	S_z
F_1	50 (±12)	3.41	4.43	29.3
F_7	35 (±10)	3.06	3.80	22.4

and the AFM images, F_7 shows a compressed, even and flatter surface in comparison with the F_1 membrane. On the contrary, the F_1 membrane illustrates a rough and uneven surface with higher roughness parameters values. Furthermore, image profile of the F_7 membrane shows a surface including the sharp and narrow pores in the membrane surface. Moreover, the coated layers modified with higher irradiation power and AA concentration show a compressed surface which refers to further cross-linking between the chitosan chains and creation a compressed structure. As seen in Fig. 4(a), the highest peak in the F_1 membrane is about 32.7 nm while it decreased to 24.9 nm for F_7 membrane (see Fig. 4(b)). On the other hand, the membrane surface pore sizes were measured using image profiles by SPM DME software. Accordingly, the mean surface pore size of F_1 membrane is 50 nm while that is 35 nm for F_7. In this

novel technique, the SPM DME software can measure the size of the pore on the basis of surface roughness. There is no measurement of the pores in the membrane matrix using this procedure. In this work, we wanted to show that the surface pores (or valleys) would be changed by AA and MW irradiation. AFM shows the significant alterations in the dark areas of the membrane surface. It clearly shows that a compressed and even layer including the small pore sizes was fabricated when the chitosan layer was modified by AA and microwave irradiation. Consequently, a surface including many dark parts was changed to create a compressed and dense surface including a few dark areas.

By the way, that is not all. Fig. 5(a) shows an SEM image of the F_7 membrane containing 4.2 wt% of AA. In spite of the formation a compressed surface (see Fig. 4(b)), our results showed many cracks and defects distributed on the chitosan surface by increasing the AA concentration. Probably, the increase of AA concentration could enhance the possibility of homopolymerization to create the polyacrylic acid chains. Hence, settling and situating of polyacrylic acid chains in the space of among CS chains causes the formation of some free volumes in the chitosan layer bulk, resulting in the creation of defects in some parts of the surface [22]. The schematic pattern of the occurred process is shown in Fig. 5(b). However, the creation of many defects in some areas of the chitosan layer struc-

Fig. 5. (a) Surface SEM image and (b) schematic of the possible mechanism.

ture affects the membrane performance, especially the rejection capability of the prepared membranes.

3. Hydrophilicity of the Surfaces

Based on the mentioned results in the previous section, we have anticipated an increase in the hydrophilicity of the coated layers due to the presence of a large number of -COOH groups [31]. As seen in Fig. 6, the hydrophilicity of the coated layers was enhanced by increasing the irradiation time. In fact, the more cross-linking process and higher number of -COOH groups in the structure of the chitosan layer as well as formation of radical sites caused a significant enhancement in the hydrophilicity. The contact angle of the PES membrane and 10s-irradiated layer was measured at 87° and 80°, respectively, which approximately decreased to about 70° for the 30s-irradiated layer. In addition, the water contact angle of the 60s-irradiated layer climbed down to 40°.

4. Performance and Antifouling Properties of the Membranes

The performance and ability of the chitosan-coated PES membranes were measured to show and investigate how the formed chitosan layer was influenced by preparation conditions. The results represented that coating of the support membrane by chitosan caused
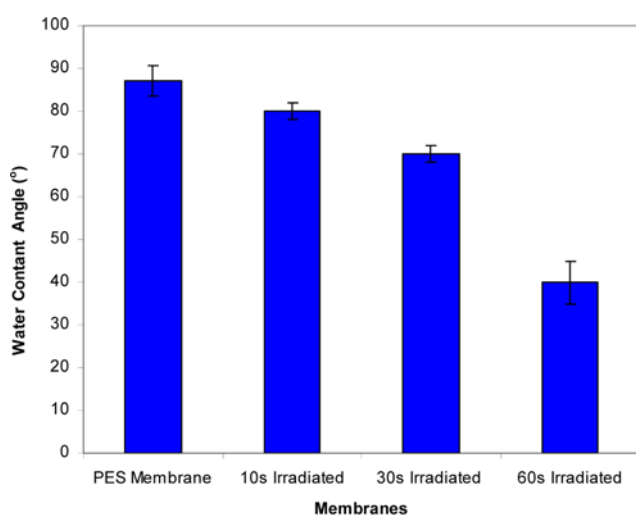
sharp decreasing in pure water flux. The pure water flux of the prepared UF membrane was measured at 165 L/m^2 h, which decreased sharply down to near 11 L/m^2 h after the formation of chitosan layer. Fig. 7 shows that the flux of the chitosan-coated PES membranes did not change significantly. Alterations in the obtained flux values of the coated membranes were very minor. For example, by increasing the irradiation power, the pure water flux increased from 10.1 L/m^2 h (180 W) to 10.5 L/m^2 h (360 W) and then decreased to 9.5 L/m^2 h (540 W), respectively. Similarly, changes in the water flux were not significant by the changes in irradiation time and AA

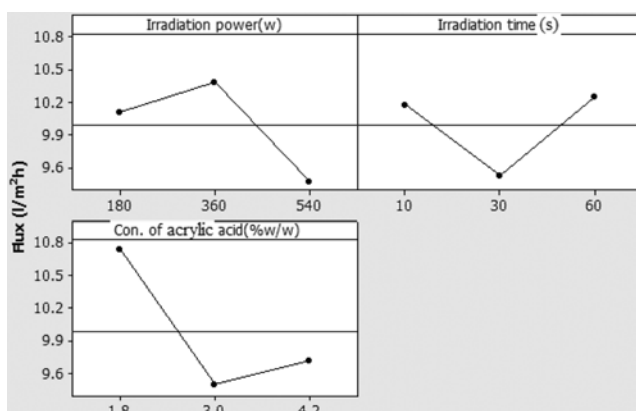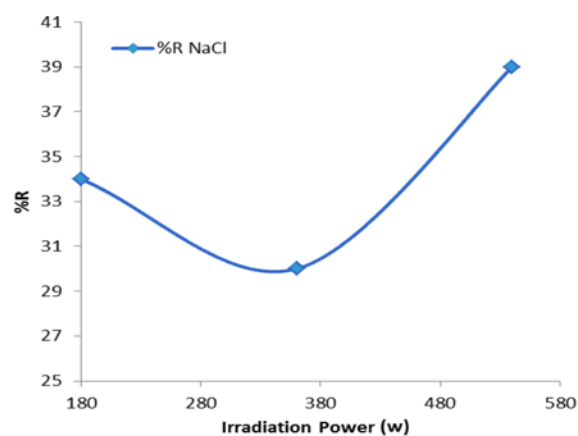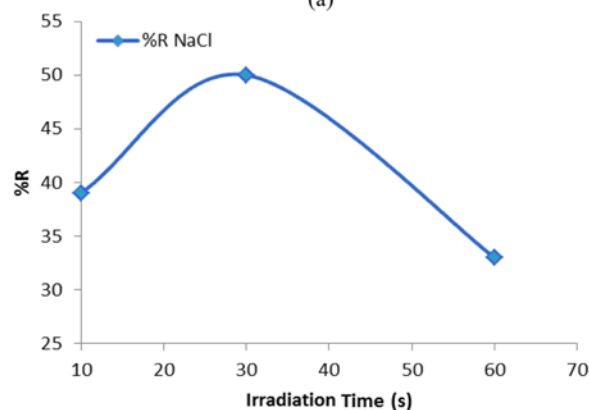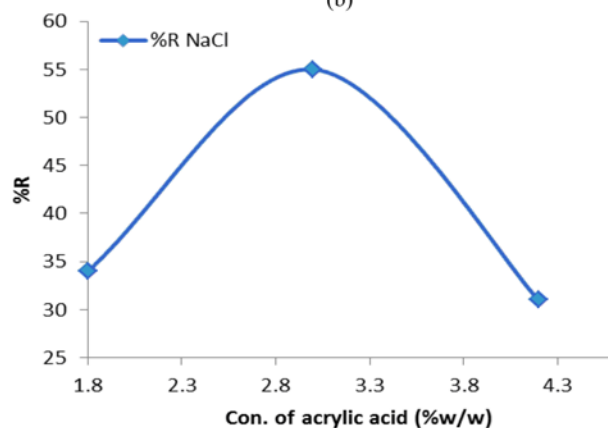Fig. 6. Water contact angle of the fabricated thin layers vs. irradiation time.

Fig. 7. Effects of irradiation power, irradiation time and AA concentration on the flux of the modified membranes.

Fig. 8. Effects of (a) irradiation power, (b) irradiation time and (c) AA concentration on the NaCl rejection.

concentration. Comparing the recent results to the older ones distinguished that the cracks distributed on the surface have not a deep height because of the insignificant changes in the flux. That is, the creation of poly acrylic acid including the -COOH groups between the chitosan chains acts as a barrier flowing; otherwise it decreases the NaCl rejection according to the Donnan exclusion theory [32, 33]. However, when the coated layers were modified by this procedure the rejection capability of prepared membranes was changed. The PES support shows the NaCl rejection about 16%. As seen in Fig. 8(a), the NaCl rejection decreased from 34% to 30% and then increased to near 40% by increasing the irradiation power from 180 to 540 W, respectively. In addition, the NaCl rejection capability of the modified layers increased from 39% to near 50% by rising irradiation time from 10 to 30 s (Fig. 8(b)). However, at 60 s the rejection capability strongly decreased to near 33%. On the other hand, changes in AA concentration from 1.8 to 3 w/v% led to significant changes in the NaCl rejection from 34% to 55%, respectively. Yet, at 4.2 w/v%, the rejection decreased to near 32% (Fig. 8(c)). According to these results, the proper conditions for having high and significant NaCl rejection were found as 540 W irradiation power, 30 s irradiation time and 3 w/v% of AA. Regarding the rejection capability of the membranes and based on the Donnan exclusion [33], we think that in the presence of AA and microwave irradiation the cross-linking process between the polymers chains increases. Under these conditions, either compressing and condensing of the polymer chains or presence of some unreacted $-NH_2$ functional groups in the structure of chitosan causes the formation of a dense layer with positively charged surface. Accordingly, the rejection capability of NaCl could be increased. But, by further increasing the modification conditions (irradiation power, irradiation time and AA concentration), higher numbers of $-NH_2$ groups might be involved in the cross-linking, resulting in a sharper decrease in the positive charge of the thin layer surface. Hence, the rejection capability of NaCl was decreased. Furthermore, in the presence of AA the number of -COOH groups was increased, resulting in decreasing of NaCl rejection [33]. As a result, a layer with smaller pore size and compressed surface was achieved. Nevertheless, the main factor affecting the NaCl rejection was the surface charge which was influenced by the presence of different functional groups. Accordingly, the effect of the changes in the pore sizes is not significant.

According to the literature, BSA (as a protein and a model) has

Table 4. Irreversible resistance, reversible resistance and flux recovery ratio of the prepared membranes

Membrane	R_{ir}	R_r	FRR
F_0	80	0.52	20
F_1	55.14	5.67	44.86
F_2	53.41	3.96	46.59
F_3	61.63	2.53	38.37
F_4	51.31	1.07	48.69
F_5	57.2	0	42.8
F_6	60	2.57	40
F_7	61	4.75	39
F_8	57.35	5.51	42.65
F_9	40	11.74	60

a superior fouling tendency, which is deposited on the surface of the membrane and gradually forms a layer upon the membrane surface [34]. For measuring the fouling tendency of the prepared thin layers, an aqueous solution of BSA with 1,000 ppm concentration was used. As seen in Fig. 9, the fouling tendency value of the F_9 membrane (40%) was half of that obtained for the F_0 thin layer (80%). The results showed that the fouling tendency of the F_0 membrane was very significant compared to the others. However, the AA-modified layers by microwave irradiation demonstrated less tendency to fouling. In addition, flux recovery ratio (FRR) of the F_9 membrane was at 60% approximately, while it was at about 20% for the F_0 membrane. As shown in Table 4, all of the modified membranes illustrated better FRR than the unmodified membrane. Fig. 10 clearly shows the flux behavior of the prepared membranes under the filtration of BSA solution during 2 h. Accordingly, the F_0 membrane depicted a remarkable decline in the flux in comparison with the modified membranes. The modified membranes, however, illustrated a little decrease in the flux. It refers to the successful modification of the chitosan-coated PES membranes to change and increase the performance.

More specifically, by increasing the AA concentration to 3 wt%, a lesser tendency to fouling could be observed (Table 4). For instance,
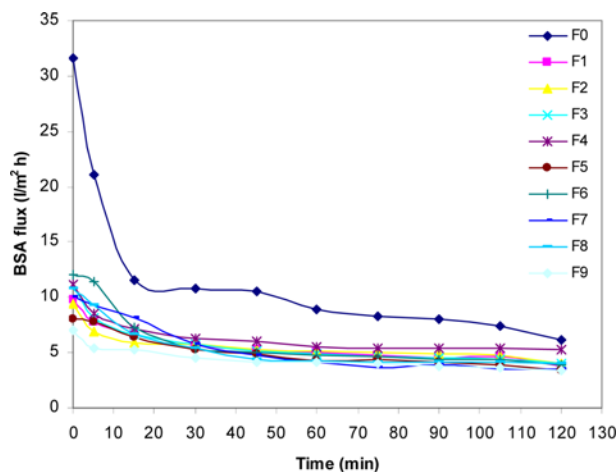
Fig. 9. Fouling tendency of the prepared thin layers.

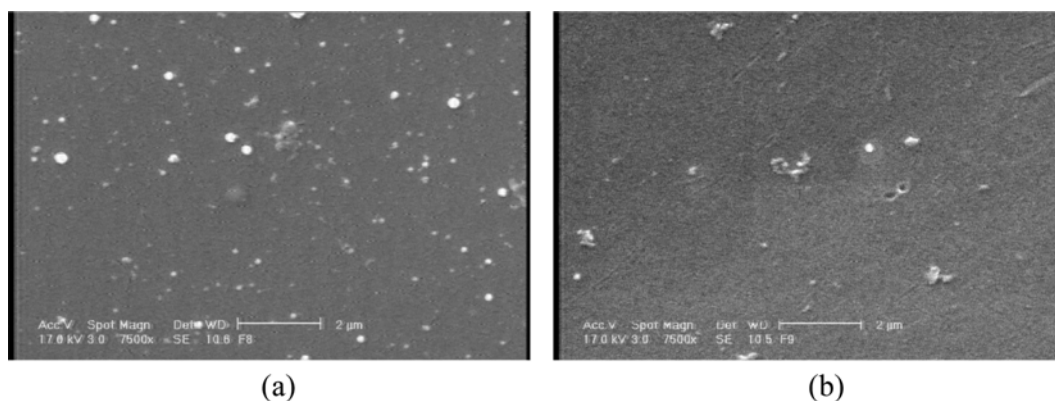**Fig. 10. Flux behavior of the membranes during BSA filtration.**

Fig. 11. SEM images of (a) F_8 and (b) F_9 thin layers.

similar irradiation power was used for the F_8 and F_9 membranes, but the AA concentration and irradiation time for the F_9 membrane were higher than those used for F_8. The results showed that the membrane fouling tendency of F_9 (40%) was lower than that of F_8 (57%). Formation of a dense and compressed layer (with less pore numbers) could be a reason to reduce the fouling. Both increasing the hydrophilicity and enhancing the number of -COOH groups could be considered as the second reason. SEM images (Fig. 11) obtained from F_8 and F_9 surfaces clearly showed that the F_9 membrane surface was more compressed and integrated than that of F_8 (see more descriptions in Fig. 4). The surfaces with even and compressed properties showed less tendency to fouling compared to the coated layers with higher porosity and uneven surface. However, a further tendency to fouling was observed at higher concentrations of AA (4.2 wt%) that, as mentioned before, could be due to the homopolymerization process and formation the cracks on the surface (see explanations of Fig. 5(a)).

Generally, the fouling tendency was reduced at a moderate concentration of AA along with increasing of irradiation time and irradiation power. In these conditions, the cross-linking process is encouraged, leading to a compressed layer including smaller pore sizes. Therefore, due to the formation a compressed layer, interpenetration of BSA molecules into the membrane matrix during the filtration process might be difficult. The compressed and even surface structure along with higher hydrophilicity of the modified thin layers reinforced the antifouling properties of the fabricated membranes.

CONCLUSION

Modification of chitosan layer by AA and microwave irradiation was introduced as a powerful and proper way to develop the coating process and enhance the performance. This study showed that the properties of chitosan layer surface were changed by increasing the irradiation power, irradiation time and AA concentration. According to the results, moderate conditions are recommended to fabricate a proper chitosan layer with enhanced properties and high NaCl rejection. The results also proved that the cross-linking process to involve functional groups is successful. By measuring the antifouling properties of the prepared thin layers, it was understood that increasing the irradiation time, irradiation power

as well as using a moderate AA concentration leads to better development of the cross-linking process, resulting in a dense layer including the smaller pore sizes. These overall led to less fouling tendency of the modified layers under filtration.

REFERENCES

1. L. Lianchao, W. Baoguo, T. Huimin, C. Tianlu and X. Jiping, *J. Membr. Sci.*, **269**, 84 (2006).
2. S. Verissimo, K. V. Peineman and J. Bordado, *J. Membr. Sci.*, **279**, 266 (2006).
3. V. Jain, H. Yochum, H. Wang, R. Montazami, M. A. V. Hurtado, A. Mendoza-Galvan, H. W. Gibson and J. R. Heflin, *Macromol. Chem. Phys.*, **209**(2), 150 (2008).
4. V. Jain, R. Sahoo, J. R. Jinschek, R. Montazami, H. M. Yochum, F. L. Beyer, A. Kumar and J. R. Heflin, *Chem. Commun.*, **31**, 3663 (2008).
5. M. A. Meyer, P. Y. Chen, A. Y. M. Lin and Y. Seki, *Prog. Mater. Sci.*, **53**, 1 (2008).
6. P. N. Sudha, *Chitin, chitosan, oligosaccharides and their derivatives*, CRC Press, London, 561 (2010).
7. L. Ilium, *Pharm. Res.*, **15**, 1326 (1998).
8. O. Felt, P. Buri and R. Gurny, *Drug. Dev. Ind. Pharm.*, **24**, 979 (1998).
9. T. Sun, W. Xie and P. Xu, *Carbohydr. Polym.*, **58**(4), 379 (2004).
10. A. Srivastava, J. Tripathy, M. Mishra and K. Behari, *J. Appl. Polym. Sci.*, **106**(2), 1353 (2007).
11. P. W. Morgan, *Condensation polymers: By interfacial and solution methods*, Interscience, New York, 19 (1965).
12. A. Yamasaki, R. K. Tyagi, A. E. Fouda, K. Jonnason and T. Matsuura, *Effect of SDS surfactant as an additive on the formation of asymmetric polysulfone membranes for gas separation*, in: I. Pinnau, B. D. Freeman (Eds.), Membrane Formation and Modification, 2000 (Chapter 6).
13. A. M. Alsari, K. C. Khulbe and T. Matsuura, *J. Membr. Sci.*, **188**, 279 (2001).
14. D. M. Wang, F. C. Lin, T. T. Wu and J. Y Lai, *J. Membr. Sci.*, **142**, 191 (1998).
15. Z.-Y. Cao, H.-C. Ge and S.-L. Lai, *Eur. Polym. J.*, **37**, 2141 (2001).
16. J. Shao, Y. M. Yang and Q.-Q. Zhong, *Polym. Degrad. Stab.*, **82**, 395 (2003).

17. R. C. Metaxas and R. J. Meredith, *Industrial microwave heating*, Peter Peregrinus Ltd., London, UK (1983).
18. T. N. Danks, *Tetrahedron Lett.*, **40**, 3957 (1999).
19. S. Vandana, N. T. Devendra, T. Ashutosh and S. Rashmi, *J. Appl. Polym. Sci.*, **95**, 820 (2005).
20. S. Vandana, T. Ashutosh, T. D. Narayan and S. Rashmi, *Polymer*, **47**, 254 (2006).
21. S. Vandana, T. Ashutosh, T. D. Narayan and S. Rashmi, *J. Appl. Polym. Sci.*, **92**, 1569 (2004).
22. Y. Mansourpanah, H. Soltani Afarani, K. Alizadeh and M. Tabatabaei, *Desalination*, **322**, 60 (2013).
23. Y. Q. Wang, Y. L. Su, X. L. Ma, Q. Sun and Z. Y. Jiang, *J. Membr. Sci.*, **283**, 440 (2006).
24. C. Gabriel, S. Gabriel, E. H. Grant, B. S. J. Halstead and D. M. P. Mingos, *Chem. Soc. Rev.*, **27**, 213 (1998).
25. S. A. Galema, *Chem. Soc. Rev.*, **26**, 233 (1997).
26. V. Singh, D. N. Tripathi, A. Tiwari and R. Sanghi, *Carbohydr. Polym.*, **65**, 35 (2006).
27. D. J. Johnson, S. A. Al Malek, B. A. M. Al-Rashdi and N. Hilal, *J. Membr. Sci.*, **389**, 486 (2012).
28. Y. Mansourpanah and E. Momeni Habili, *J. Membr. Sci.*, **430**, 158 (2013).
29. N. Hilal, L. Al-Khatib, B. P. Atkin, V. Kochkodan and N. Potapchenko, *Desalination*, **158**, 65 (2003).
30. Y. Mansourpanah and Z. Amiri, *Desalination*, **335**, 33 (2014).
31. A. A. Abuhabib, A. W. Mohammad, N. Hilal, R. A. Rahman and A. H. Shafie, *Desalination*, **295**, 16 (2012).
32. Y. Mansourpanah, S. S. Madaeni and A. Rahimpour, *J. Membr. Sci.*, **343**, 219 (2009).
33. M. Y. Jeon, S. H. Yoo and C. K. Kim, *J. Membr. Sci.*, **313**, 242 (2008).
34. D. Rana and T. Matsuura, *Chem. Rev.*, **110**, 2448 (2010).